Journal of Magnetic Resonance **140,** 228–234 (1999)
Article ID jmre.1999.1799, available online at http://www.idealibrary.com on IDEAL®

Application of Multiple Inversion Recovery for Suppression of Macromolecule Resonances in Short Echo Time ^{1}H NMR Spectroscopy of Human Brain

Jack Knight-Scott

Department of Radiology, University of Virginia Health Sciences Center, Charlottesville, Virginia 22908

Received March 1, 1999; revised April 1, 1999

Macromolecules contribute broad "background" resonances to the ^{1}H NMR brain spectra at short echo times. The application of long echo times is the most widely used method for removing these resonances. Here, it is demonstrated that these background resonances may be suppressed at short echo times using multiple inversion recovery (MIR). In the technique presented, the MIR sequence consists of four adiabatic inversion pulses, applied preparatory to a 20-ms echo time stimulated echo localization sequence. The inversion times (359, 157, 69, and 20 ms) were selected to preferentially suppress macromolecules with longitudinal relaxation times between 38 and 300 ms. While the resulting spectra have lower overall signal-to-noise, baseline contributions from macromolecules are greatly reduced. Unlike the typical long TE acquisitions, the short TE MIR acquisition preserves the *myo*-inositol resonance.

Key Words: **magnetic resonance spectroscopy; proton; brain; macromolecules; suppression.**

INTRODUCTION

High molecular weight chemicals contribute broad "background" resonances to ^{1}H NMR brain spectra at short echo times (*1, 2*), making accurate identification of the baseline problematic for both absolute and relative quantitative measurements. Because the so-called "baseline distortions" created by these macromolecules have short transverse relaxation times (T_2), long echo time (TE) spectroscopy has become the most widely used technique for removing these broad resonances. The work presented here offers a method for suppressing these baseline distortions at short TEs. The method utilizes multiple inversion recovery (*3*) to suppress signal contributions over a specific range of spin–lattice relaxation times (T_1).

Dixon *et al.* first introduced multiple inversion recovery (MIR) nearly a decade ago as a method for suppressing static tissue in spin-labeled angiography (*3*). Recently, MIR has been used to selectively image gray or white brain matter (*4*), improve suppression of CSF in brain imaging (*5*), and suppress the signal from the thorax tissues in ^{1}H lung imaging (*6*). In spectroscopy, MIR has been employed to improve water suppression *in vivo* (*7*). Here, it is demonstrated that by using a MIR preparation, the magnetization from macromolecules can be selectively suppressed in short TE localized ^{1}H spectroscopy. The method is demonstrated *in vivo* for STEAM localization in human brain.

EXPERIMENTAL

Technique and Theory

A general theory of multiple inversion recovery has been thoroughly explored, both analytically and conceptually, by Dixon *et al.* (*3*) and therefore will not be discussed in detail in this paper. In the original application of the MIR technique, a saturation pulse initializes the longitudinal magnetization to the same intensity prior to application of the inversion pulses. The saturation pulse is not employed in this implementation of a combined MIR and stimulated echo localization sequence (STEAM (*8–10*)). Hence, saturation effects must be considered in the solution to Bloch equations (*11*) for the MIR-STEAM combination. A general steady-state solution to the Bloch equations for the longitudinal magnetization of a MIR-STEAM combination with N number of inversions, assuming ideal conditions, is given by

$$M_{Z\_n}(\tau) = M_{O\_n}\left\{1 + 2\sum_{i=1}^{N}\left[(-1)^i \exp\left(-\frac{\sum_{j=N-i+1}^{N}\tau_j}{T_{1\_n}}\right)\right] + (-1)^{N+1}\exp\left(-\frac{\mathrm{TR} - \mathrm{TM} - \mathrm{TE}/2}{T_{1\_n}}\right)\right\}, \quad [1]$$

where n is the T_1 species number, ranging from 1 to N; M_{Z_n}, M_{O_n}, and T_{1_n} are the longitudinal magnetization, thermal equilibrium magnetization, and T_1 of the nth T_1 species to be nulled, respectively; τ_j is the inversion time after the jth inversion pulse; τ is the total preparation time $\sum_{j=1}^{N}\tau_j$; TR is the repetition time; and TM is the mixing time. MIR manipulates the spin system so that the residual longitudinal magnetization from each of the N number of T_1 species is zero at the

1090-7807/99 $30.00

TABLE 1
Nulled T_1 Values and Inversion Times for a Four-Pulse MIR

n	T_{1_n} (ms)	τ_n (ms)
1	300	359
2	150	157
3	75	69
4	37.5	20

initiation of spectroscopic localization. Gradient spoiling is used to reduce signal contributions from transverse magnetization inadvertently created by application of the inversion pulses.

The use of nonselective RF pulses in the MIR preparation sequence will null the signals from the T_1 species of interest over the entire frequency bandwidth of the inversion pulses. The specific T_1 values and the number of nulled T_1 species are determined by the choices for T_{1_n} and N when solving for the inversion times in Eq. [1]. However, as demonstrated by other groups (*3*, *12*), MIR will not only null the signals for the specified T_1's, but will also act as a T_1-dependent broadband suppression technique. The profile of this suppression band is determined by the inversion times and number of inversion pulses. In the case of macromolecules, it is desired that short T_1 species be more greatly suppressed than long T_1 species. This can be achieved by preferential nulling of short T_1 species over a specified range of T_1 values, ΔT_1.

To suppress macromolecule resonances for a specific N number of T_1 values, it is required that all N sets of Eq. [1] be simultaneously solved for the inversion times τ_j that make the sum of the absolute values of the longitudinal magnetization equal to zero at time τ, $\sum_{n=1}^{N} |M_{Z\_n}(\tau)| = 0$. These sets of equations can be solved easily and exactly for $N = 1$ or 2. However, for larger values of N, the inversion times are best determined through numerical optimization using a standard iterative minimization or search algorithm.

Sequence Parameters and Computer Simulation

Solving Eq. [1] for the inversion times requires preselection of TE, TR, TM, N, and the specific T_{1_n} values. The T_{1_n} values were chosen to suppress signal contributions from T_1 species between 38 and 300 ms for $N = 4$. As recently demonstrated by Hofmann *et al.* (*13*), this range includes many of the macromolecule resonances that are typically identified as baseline distortions. The selected T_{1_n} values are shown in Table 1. The τ_n values were determined from a solution to Eq. [1] using a Marquardt–Levenberg nonlinear least-squares algorithm provided in SigmaPlot (SPSS Inc., Chicago, IL). The τ_n values were constrained to positive times between $\tau_n > 10$ ms and $\sum_{i=1}^{4} \tau_n = \tau <$ TR–TE–TM. The normalized magnetization was simulated as a function of T_1, using Eq. [1], to examine the suppression profile for the inversion times shown in Table 1.

In Vivo Experiments

All experiments were performed on a 1.5-T Magnetom Vison whole-body MRI system (Siemens Medical Systems, Iselin, NJ) using a Siemens standard 27-cm circularly polarized proton head coil. All human studies were performed under a protocol approved by the institutional review board and under the informed and written consent of each volunteer.

The MIR preparation sequence consisted of four 10-ms hyperbolic secant pulses each followed by a 2-mT/m gradient pulse of variable length (dependent upon the inversion time). Water suppression was performed by RF saturation and gradient spoiling of the water magnetization during the third inversion period using a single 26-ms frequency selective Gaussian pulse (bandwidth 50 Hz) followed by a 10-ms 2-mT/m sinusoidal gradient. The MIR-STEAM sequence parameters were TE/TM/TR = 20/10/4000 ms. A diagram of the MIR-STEAM sequence is shown in Fig. 1 without the water suppression sequence. Data acquisition time was 819.2 ms for 1024 complex data points. The localization RF pulses were alternated through an eight-step phase cycle to reduce outer volume contamination and spectral distortions.

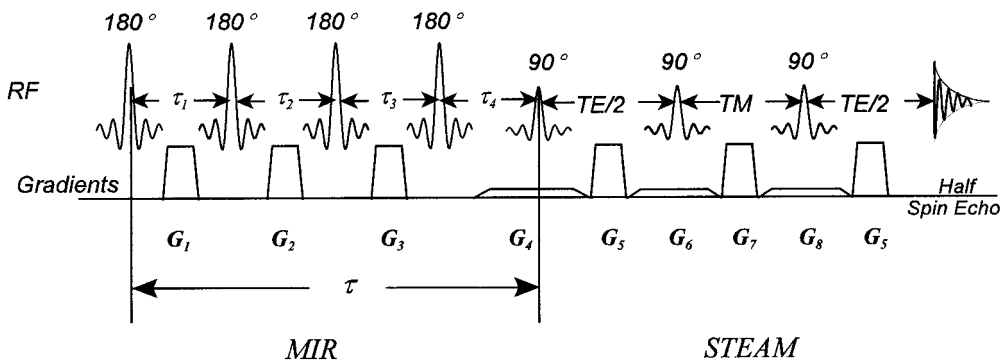

FIG. 1. A four-pulse MIR preparation sequence combined with a spectroscopic STEAM localization sequence. Total inversion time τ is equal to the sum of the individual inversion times, $\sum_{i=1}^{4} \tau_i$. Gradient pulses $\mathbf{G}_1$, $\mathbf{G}_2$, $\mathbf{G}_3$, $\mathbf{G}_5$, and $\mathbf{G}_7$ are spoiling gradients applied along multiple orthogonal axes. $\mathbf{G}_4$, $\mathbf{G}_6$, and $\mathbf{G}_8$ are orthogonal slice selective gradients for x, y, and z axes, respectively.

^{1}H spectroscopic brain examinations were carried out on eight healthy volunteers (four males and four females, ages 21–44). Localization was performed in the hippocampus, parietal lobe, or occipital lobe. Volumes varied from 5 to 10 cm^3. Each examination included a MIR-1-STEAM, and a 3-DRYSTEAM (TE/TM/TR = 20/10/4000 ms) acquisition. If tolerated by the volunteer, a double echo localization experiment (PRESS) (*14*) was also performed using a 3-DRYPRESS (TE/TR = 135/4000 ms) sequence (see Ref. *15* for nomenclature for localization sequences). All water-suppressed data were averaged 128 times. An unsuppressed water reference was acquired with each data set. In a separate examination, a 14-point T_2 measurement (15-s TR, 26 to 1000-ms TE's, no averaging) for unsuppressed water was performed on one of the volunteers to examine the effect of the MIR preparation sequence on a well-known case of multiexponential relaxation.

All data were zero-filled to 4 K, corrected for a DC offset, apodized with a Gaussian filter (water-suppressed data) or a Lorentzian filter (unsuppressed water data), and phase corrected using the water referencing method prior to FFT. The integrated area of the unsuppressed water data was obtained from a fit with a Lorentzian distribution. The T_2 data were fitted with a biexponential relaxation model using the nonlinear Marquardt–Levenberg least-squares algorithm provided in SigmaPlot.

RESULTS

All spectra were normalized to the intensity of the peak from the *N*-acetyl-aspartate (NAA) CH_3 group at 2.02 ppm. Figure 2 shows representative MIR-1-STEAM, 3-DRYSTEAM, and 3-DRYPRESS spectra acquired from the occipital–parietal region of a healthy volunteer. Figure 3 shows representative MIR-1-STEAM and 3-DRYSTEAM spectra acquired from the hippocampus of a healthy volunteer. These two data sets demonstrate the range of baseline distortions possible in typical short TE ^{1}H NMR spectra *in vivo* and show the improvements possible with a MIR-based sequence.

In the occipital–parietal data set, all three spectra reveal excellent water suppression with the metabolites peaks being easily differentiated from the residual water. The reference lines, the baselines measured by averaging the first and last 512 data points in the spectra, are represented by dashed lines. In spite of the small baseline roll in the long TE 3-DRYPRESS spectrum, baseline distortions are clearly reduced relative to the 3-DRYSTEAM spectrum. The long TE 3-DRYPRESS spectrum has only a slight sloping baseline in the 3- to 5-ppm region, while the short TE 3-DRYSTEAM spectrum reveals a much greater degree of contamination from residual water and short T_2 species. In the MIR-1-STEAM spectrum, the baseline contributions from macromolecules are clearly reduced relative to the 3-DRYSTEAM spectrum. If the *N*-acetyl (NA) peak at 2.02 ppm is triangulated, the base of the peak is coincident with the reference line, while the base of the creatine + phosphocreatine (Cre) and choline (Cho) peaks are only slightly elevated above the reference line, relative to the 3-DRYPRESS spectrum. However, whereas the *myo*-inositol (Ino) peak at 3.56 ppm is nearly absent in the 3-DRYPRESS spectrum and poorly resolved in the 3-DRYSTEAM spectrum, the peak is well resolved and easily identifiable in the MIR-1-STEAM spectrum. The Cre peak from the CH_2 group (3.9 ppm) is highly elevated in the 3-DRYSTEAM spectrum due to underlying macromolecules and residual water. Resonances underlying this peak are well suppressed in the MIR-1-STEAM and 3-DRYPRESS spectra. Overall, the MIR-1-STEAM suppresses the broad resonances that are apparent throughout

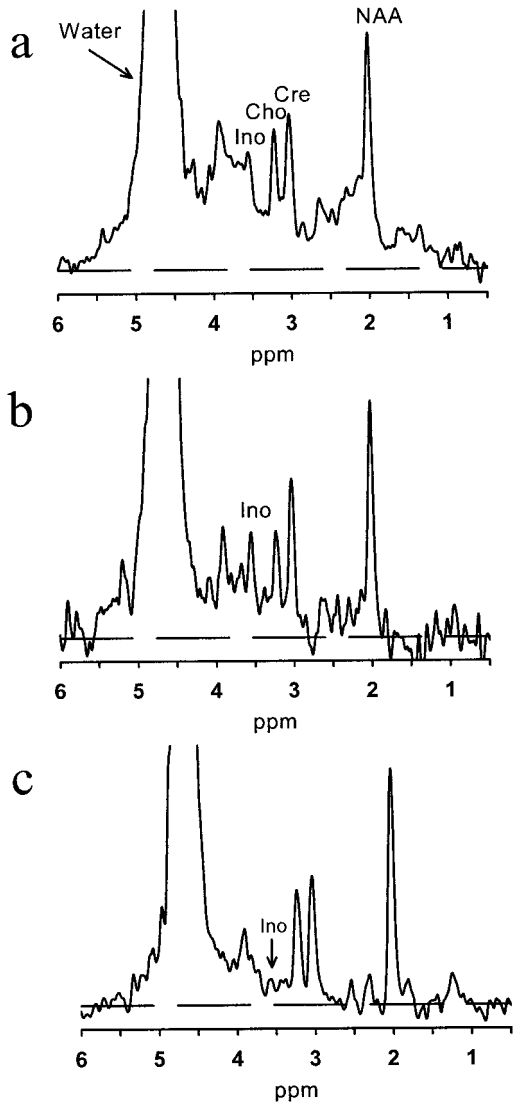

FIG. 2. (a) 20-ms TE 3-DRYSTEAM, (b) 20-ms TE MIR-1-STEAM, and (c) 135-ms TE 3-DRYPRESS spectra acquired from a 1.8 × 2 × 1.8-cm volume localized in the occipital–parietal region of a healthy volunteer. All spectra were averaged 128 times using a 4000-ms TR.

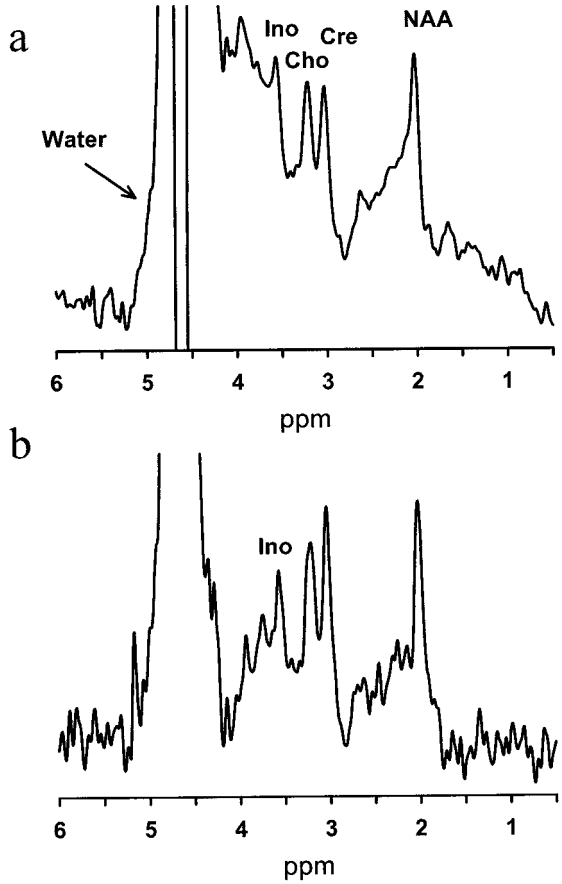

FIG. 3. (a) 20-ms TE 3-DRYSTEAM, and (b) 20-ms TE MIR-1-STEAM spectra acquired from a 2 × 2 × 1.8-cm volume localized on the right hippocampus of a healthy volunteer. All spectra were averaged 128 times using a 4000-ms TR.

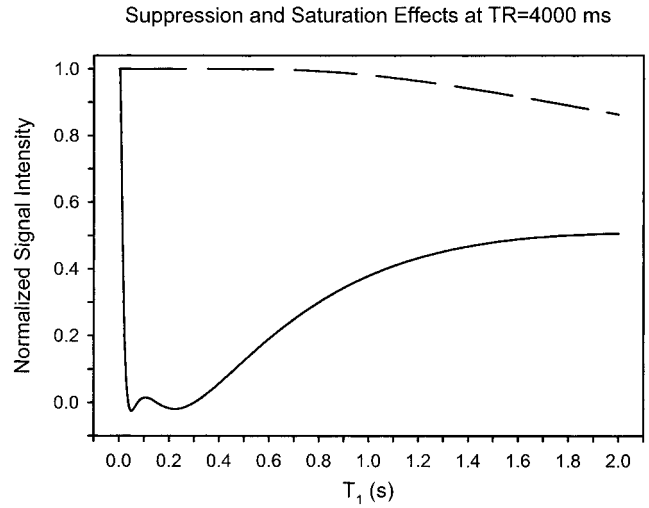

FIG. 4. Suppression profile (solid line) and saturation curve (dashed line) as a function of T_1 for a four-pulse MIR-STEAM acquisition for TE/TM/TR = 20/10/4000 ms. Inversion times are given in Table 1. Curves have been normalized relative to the thermal equilibrium magnetization $M_0(T_1)$.

the standard short TE 3-DRYSTEAM spectrum, while preserving many of the narrower resonances.

Short TE spectra from the hippocampus usually exhibit extreme baseline distortions, due to significant contributions from macromolecules and increased B_0-field inhomogeneities in this region, as is evident in Fig. 3a. Suppressing the macromolecule resonances through multiple inversion recovery removes most of the baseline distortions. In particular, the large sloping baseline extending from the water resonance to about 0.5 ppm is absent from the MIR-STEAM spectrum (Fig. 3b). The resolution of the spectrum is clearly improved.

These two data sets demonstrate how great the regional differences in baselines can be. Because the baseline and the suppression efficiency ε of MIR are functions of T_1, the results of MIR-based sequences are highly region dependent. Figure 4 shows the simulated suppression profile of a MIR-STEAM sequence as a function of T_1 using the parameters given in Table 1. Theoretically, ε for T_1 species between 30 and 300 ms is 97% or greater, while for T_1 species between 900 and 1500 ms—the range of T_1 values for the major ^{1}H metabolites *in vivo*—ε is between 50 and 70%. The suppression efficiency is given empirically by

$$\varepsilon = 100\%\left[1 - \frac{S(\text{MIR-1-STEAM})}{S(3-\text{DRYSTEAM})}\right] \qquad [2]$$

for long TR values, where S is the signal intensity from the MIR-1-STEAM or 3-DRYSTEAM experiment. By substituting the measured ε into Eq. [1], and the equation describing the signal from a standard STEAM acquisition (*16*), a "bulk T_1" value $\overline{T_1}$ can be determined. Because the residual water and macromolecules are not removed from the spectra, the peak amplitude of the metabolites is used to calculate ε and avoid the baseline identification problem associated with many line fitting algorithms (*17*). The resulting ε and $\overline{T_1}$ values are summarized in Table 2.

As expected, the $\overline{T_1}$ values for NA, Cre, Cho, Ino, and water resonances are less than many previously reported values (*18–24*). Contributions from macromolecules yield $\overline{T_1}$'s with aver-

TABLE 2
Average MIR Suppression Efficiency and $\overline{T_1}$ Values from Eight Healthy Volunteers

Resonance	ε (%) (mean ± std. dev.)	$\bar{T}_1$ (ms) (mean ± std. dev.)
NA	0.59 ± 0.04	1084 ± 121
Cre	0.60 ± 0.03	1035 ± 86
Cho	0.63 ± 0.06	967 ± 156
Ino	0.63 ± 0.08	982 ± 253
Water	0.72 ± 0.06	757 ± 123

age T_1 values shorter than those of the metabolites. The large coefficient of variance (CV) for the $\overline{T_1}$ of the metabolites, mean = 15.4%, reflects differences in water suppression efficiency and regional concentration, as well as differences in the relative signal contributions from macromolecules. Unsurprisingly, Ino has the largest CV (~25%), mirroring published results that reveal regional T_1 differences of up to 50% (*18, 20*).

The metabolite ε values vary from a low of 51% to a high of 73% (mean: 61 ± 6%), in excellent agreement with the predicted range. Nonetheless, these values are probably greater than the true metabolite ε values, since part of the loss in signal amplitude is due to the suppression of underlying macromolecules. With an average $\varepsilon \sim 72 \pm 6\%$, the water is moderately suppressed by the MIR preparation sequence. This allows the use of only one RF pulse for water suppression.

The effects of MIR on the water signal can also be seen by comparing the acquired T_2 curves (Fig. 5). In a biexponential fit, the water signal is assumed to be bicomponent. In tissue, the primary component has a short T_2, T_{2S}, of less than 100 ms, while the second component has a long T_2, T_{2L}, ranging between 200 and 2000 ms (*25*). The MIR-STEAM acquisition exhibits an overall longer T_2 than the standard STEAM acquisition, as well as an increase in the relative signal contribution from the long T_2 component (Table 3). The removal of short T_1 water components concomitantly reduces contributions from short T_2 components, resulting in a relative increase in contributions from the long T_2 components.

TABLE 3
Water Transverse Relaxation Times for a Healthy Volunteer

Biexponential fit parameters	MIR-STEAM (mean ± std. dev.)	DRYSTEAM (mean ± std. dev.)
T_{2S} (ms)	76.8 ± 1.4	75.3 ± 0.7
T_{2L} (ms)	563.7 ± 53.6	486.5 ± 80.4
$M_0(T_{2S})^a$	1.19 ± 0.01	1.34 ± 0.01
$M_0(T_{2L})^a$	0.16 ± 0.01	0.05 ± 0.01

[a] Values have been normalized to signal intensity from the 20-ms TE acquisition.

DISCUSSION

The primary advantage of long TE ^{1}H NMR spectroscopy *in vivo* is that the subsequent flat baselines make identification and quantitation of the resonances relatively simple. However, at typical TEs of 135 ms or greater, the severe T_2 weighting of the technique drastically reduces the information content of the spectra, thus reducing the sensitivity and specificity of ^{1}H spectroscopy. Multiple inversion recovery spectroscopy sequences have the potential to significantly suppress baseline artifacts while keeping the information content of spectra high. In the previous examples shown, the MIR-1-STEAM dramatically improves the baselines at a short TE. In brain regions where contributions from macromolecules are especially high, such as in the hippocampus, where recent studies suggest a 20% failure rate for acquisitions from healthy normal volunteers (*26*), a MIR-based sequence may be particularly useful.

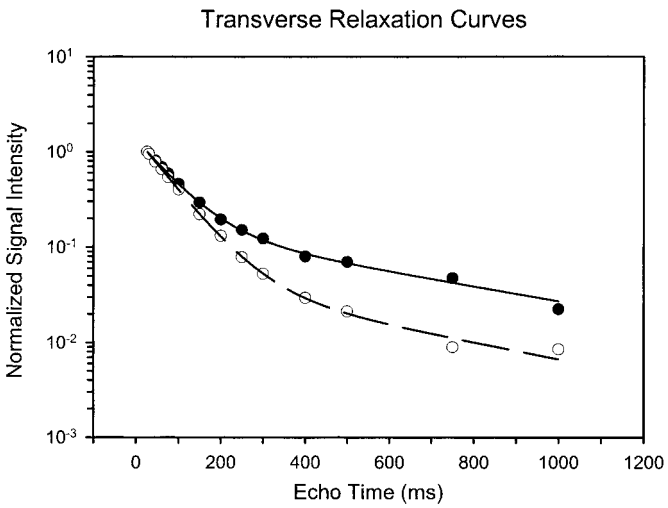

FIG. 5. A semi-log plot of normalized T_2 curves for water in the human brain. Data points are represented by (●) for the MIR-STEAM curve and (○) for DRYSTEAM, while the results of the respective biexponential fits are represented by a solid line and a dashed line.

For suppressing the macromolecules, ΔT_1 has to be preselected. Unfortunately, there are little T_1 data for macromolecules at 1.5 T. The choice in this case was based mainly on the graphical data of Hofmann *et al.* (*13*). The lower threshold value of 30 ms was selected to keep the minimum inversion time above 20 ms, the shortest interval possible that would still allow adequate time for gradient spoiling on the MRI system. The upper value of 300 ms was selected to allow the magnetization at 4000 ms TR to recover to approximately 37% (one time constant) of its steady-state value for T_1 = 900 ms, the shortest T_1 usually reported for ^{1}H metabolites *in vivo.* However, without full T_1 characterization of the macromolecule spectrum, it is unknown whether this selected ΔT_1 is the most appropriate choice. Further experiments are necessary to measure the suppression factor for the macromolecule spectrum.

The most critical drawback of MIR is the reduction in signal intensity. In some aspects this complicates absolute quantitation methods. Because MIR spectra are highly T_1-weighted, they must be corrected for T_1-dependent signal loss due to the multiple inversions. A long TR is no longer sufficient for removing T_1 weighting. Since a MIR preparation tends to reduce overall spectral SNR, it is crucial that the sequence be optimized to yield (i) minimum signal intensity over ΔT_1, and (ii) maximum SNR over a selected range of T_1 values outside the suppression region. In the current MIR-1-STEAM implementation, the sequence is only optimized to minimize the signal intensity over the selected ΔT_1. The overall spectral SNR is roughly comparable to a 150-ms TE STEAM acquisi-

tion. One method for improving the SNR is by using a different localization scheme. A doubling of the SNR may be easily gained through a short TE MIR-PRESS acquisition. It may also be possible to increase the SNR by improving the suppression profile. For example, the B_1- and T_1-insensitive water-suppression method WET (*12*) is a solution to the same suppression problem proposed by Dixon *et al.* (*3*). Both WET and MIR attempt to manipulate the evolution of the spin system such that the residual longitudinal magnetization over a specified T_1 range or specific T_1 values is zero at the initiation of spectroscopic localization or imaging. In MIR, the flip angles of the preparatory RF pulses are fixed to 180°, and the delay time between the RF pulses is allowed to vary. In contrast, the flip angles are the variables in implementing the WET technique, while the delay times are fixed at a prechosen value. By allowing both the flip angles and the delay times to vary for the solution, it might be possible to reduce suppression effects for chemicals with T_1 values outside the selected ΔT_1 if the suppression profile can be closely matched to that of a step function.

The simulated suppression profile shows oscillations on the order of $\pm 3\%$ over ΔT_1. These variations are not expected to greatly affect the spectral pattern if originating from the residual macromolecule signals. In regions of high macromolecule concentrations or poor B_0-field homogeneity, these oscillations will likely increase the overall variance and could possibly be mistaken for a pathological-dependent spectral alteration. A different MIR scheme might reduce the intensity of these oscillations.

An unanticipated advantage of MIR is that it simplifies water suppression by reducing the number of T_1 components. For typical water suppression sequences, as one tries to minimize the residual water signal, the observed peak will frequently split, part positive and part negative. Because of multiexponential relaxation, for some regions of the brain it is not possible to simultaneously suppress the various components of the water with the standard three RF pulses permutation (*27*). The MIR preparation sequence reduces the water signal by 70%, so that when using only a single frequency selective water suppression RF pulse, water-suppression factors less than 200:1 (relative to the NA resonance) can be achieved. Additional frequency selective RF pulses, interleaved within MIR, may yield further reductions in the water-suppression factor.

MIR-based sequences may also be advantageous in other spectroscopic techniques. For instance, a major drawback of *me*tabolite *nu*lling (MENU (*1, 2*)) is that it assumes a single T_1 for all the metabolites of interest. A MIR scheme could simultaneously null metabolites for three or more T_1 values. It would be fairly simple to simultaneously null the NA, Cre, Cho, and Ino resonances. Even a simple double-inversion scheme would yield improved results by widening the T_1 suppression range. MIR could also be applied to ^{1}H spectroscopic imaging (HSI). HSI methods that acquire at least a complete slice must suppress the signal from the subcutaneous fat of the scalp. The two most widely used techniques are HSI combined with a single-voxel localization sequence and HSI combined with outer volume saturation (OVS) (*28*). The single-voxel technique limits the region of interest to only tissue definitively within the scalp borders. OVS attempts to saturate the fat signal from the scalp, prior to slice excitation and phase encoding. These techniques could be replaced by MIR, optimized to yield very efficient fat suppression.

CONCLUSIONS

In preliminary studies, it has been shown that baseline distortions due to chemicals with short spin–lattice relaxation times can be suppressed in short echo time ^{1}H brain spectra through selective T_1 weighting using a multiple inversion recovery preparation sequence. Preliminary results show spectra with only minor baseline distortions at a 20-ms TE. There is an unavoidable reduction in signal intensity similar to that of long echo time spectroscopy studies. In comparison to the long TE studies, the overall spectral information content is not as greatly reduced. Specifically, the *myo*-inositol resonance is preserved.

Multiple inversion recovery appears to be a promising technique that may widely impact MR spectroscopy. The results presented here establish the basic concepts of MIR for localized spectroscopy. Additional studies are necessary to quantitate MIR-based spectra, perform large scale statistical studies, reexamine peak identification due to the improvement in resolution, and optimize the suppression profile.

ACKNOWLEDGMENTS

I am indebted to Vu M. Mai for coercing me into collaborating with him, Siemens Medical System for their financial support, Shella Keilholz-George for her editing skills, and the many volunteers who endured my spectroscopy examinations.

REFERENCES

1. K. L. Behar, D. L. Rothman, D. D. Spencer, and O. A. C. Petroff, Analysis of macromolecule resonances in ^{1}H NMR spectra of human brain, *Magn. Reson. Med.* **32,** 294–302 (1994).
2. K. L. Behar and T. Ogino, Characterization of macromolecules resonances in the ^{1}H NMR spectrum of rat brain, *Magn. Reson. Med.* **30,** 38–44 (1993).
3. W. T. Dixon, M. Sardashti, M. Castillo, and G. P. Stomp, Multiple inversion recovery reduces static tissue signal in angiograms, *Magn. Reson. Med.* **18,** 257–268 (1991).
4. T. W. Redpath and F. W. Smith, Technical note: Use of a double inversion recovery pulse sequence to image selectively gray or white brain matter, *Br. J. Radiol.* **67,** 1258–1263 (1994).
5. K. Turetschek, P. Wunderbaldinger, A. A. Bankier, T. Zontsich, O. Graf, R. Mallek, and K. Hittmair, Double inversion recovery imaging of the brain: Initial experience and comparison with fluid attenuated

inversion recovery imaging, *Magn. Reson. Imaging* **16,** 127–1135 (1998).

6. V. M. Mai, J. Knight-Scott, and S. S. Berr, Improved visualization of the human lung in ^{1}H MRI using multiple inversion recovery to simultaneously suppress signal contributions from fat and muscle, *Magn. Reson. Med.* **41,** 866–870 (1999).
7. J. F. Shen and J. K. Saunders, Double inversion recovery improves water suppression in vivo, *Magn. Reson. Med.* **29,** 540–542 (1993).
8. J. Granot, Selected volume excitation using stimulated echoes (VEST). Application to spatially localized spectroscopy and imaging, *J. Magn. Reson.* **70,** 488–492 (1986).
9. R. Kimmich and D. Hoepfel, Volume-selective multipulse spin-echo spectroscopy, *J. Magn. Reson.* **72,** 379–384 (1987).
10. J. Frahms, K-D. Merboldt, and W. Hänicke, Localized proton spectroscopy using stimulated echoes, *J. Magn. Reson.* **72,** 502–508 (1987).
11. F. Bloch, Nuclear Induction, *Phys. Rev.* **70,** 460–474 (1946).
12. R. J. Ogg, P. B. Kingsley, and J. S. Taylor, WET, a T_1- and B_1-insensitive water-suppression method for *in vivo* localized ^{1}H NMR spectroscopy, *J. Magn. Reson. B* **104,** 1–10 (1994).
13. L. Hofmann, J. Slotboom, C. Boesch, and R. Kreis, Improved definition of baseline in localized ^{1}H-MRS based on T_1-differences, *in* "Proceedings of the International Society for Magnetic Resonance in Medicine, 6th Scientific Meeting, Sydney, Australia, April 18–24, 1998," p. 1853.
14. P. A. Bottomley, Spatial localization in NMR spectroscopy, *Ann. N.Y. Acad. Sci.* **508,** 333–348 (1987).
15. C. T. W. Moonen, and P. C. M. Van Zijl, Highly effective water suppression for *in vivo* proton NMR spectroscopy (DRYSTEAM), *J. Magn. Reson.* **88,** 28–41 (1990).
16. J. Knight-Scott and S-J. Li, Effect of long TE on T_1 measurement in STEAM progressive saturation experiment, *J. Magn. Reson.* **126,** 266–269 (1997).
17. P. S. Tofts and S. Wray, A critical assessment of methods of measuring metabolite concentrations by NMR spectroscopy, *NMR Biomed.* **1,** 1–10 (1988).
18. J. Frahm, H. Bruhn, M. L. Gyngell, K-D. Merboldt, W. Hänicke, and R. Sauter, Localized proton NMR spectroscopy in different regions of the human brain *in vivo.* Relaxation times and concentrations of cerebral metabolites, *Magn. Reson. Med.* **11,** 47–63 (1989).
19. P. A. Narayana, D. Johnston, and D. P. Famig, *In vivo* proton magnetic resonance spectroscopy studies of human brain, *Magn. Reson. Imaging* **9,** 303–308 (1991).
20. R. Kreis, T. Ernst, and B. D. Ross, Absolute quantification of water and metabolites in the human brain. II. Metabolites concentrations, *J. Magn. Reson. B* **102,** 9–19 (1993).
21. P. Christiansen, P. Toft, H. B. W. Larsson, M. Stubgaard, and O. Henriksen, The concentration of *N*-acetyl aspartate, creatine + phosphocreatine, and choline in different parts of the brain in adulthood and senium, *Magn. Reson. Imaging* **11,** 799–806 (1993).
22. P. Christiansen, O. Henriksen, M. Stubgaard, P. Gideon, and H. B. W. Larsson, *In vivo* quantification of brain metabolites by ^{1}H-MRS using water as an internal standard, *Magn. Reson. Imaging* **11,** 107–118 (1993).
23. P. Christiansen, A. Schlosser, and O. Henriksen, Reduced *N*-acetylaspartate content in the frontal part of the brain in patients with probable Alzheimer's disease, *Magn. Reson. Imaging* **13,** 457–462 (1995).
24. D. J. Manton, M. Lowry, S. J. Blackband, and A. Horsman, Determination of proton metabolites concentrations and relaxation parameters in normal brain and intracranial tumours, *NMR Biomed.* **8,** 104–112 (1995).
25. T. Ernst, R. Kreis, and B. D. Ross, Absolute quantification of water and metabolites in the human brain. I. Compartments and water, *J. Magn. Reson. B* **102,** 1–8 (1993).
26. C. G. Choi and J. Frahm, Localized proton MRS of the human hippocampus: Metabolite concentrations and relaxation times, *Magn. Reson. Med.* **41,** 204–207 (1999).
27. T. Ernst and J. Hennig, Improved water suppression for localized *in vivo* ^{1}H spectroscopy, *J. Magn. Reson. B* **106,** 181–186 (1995).
28. J. H. Duyn, J. Gillen, G. Sobering, P. C. M. Van Zijl and C. T. W. Moonen, Multisection proton MR spectroscopic imaging of the brain, *Radiology* **188,** 277–282 (1993).